Bull Volcanol (2011) 73:133–142
DOI 10.1007/s00445-010-0438-8

RESEARCH ARTICLE

Seismicity and magma supply rate of the 1998 failed eruption at Iwate volcano, Japan

Takeshi Nishimura · Sadato Ueki

Received: 15 January 2010 / Accepted: 1 December 2010 / Published online: 18 February 2011
© Springer-Verlag 2011

Abstract Iwate volcano, Japan, showed significant volcanic activity including earthquake swarms and volcano inflation from the beginning of 1998. A large earthquake of magnitude 6.1 hit the south-west of the volcano on September 3. Although a 1 km^2 fumarole field formed, blighting plants on the ridge in the western part of the volcano in the spring of 1999, no magmatic eruptions occurred. We reconcile the spatio-temporal distributions of volcanic pressure sources determined by previously reported studies in which GPS, strain and tilt data from dense geodetic station networks are analyzed (Miura et al. Earth Planet Space 52:1003–1008, 2000; Sato and Hamaguchi J Volcanol Geotherm Res 155:244–262, 2006). We calculate the magma supply rates from their results and compare them with the occurrence rates of volcanic earthquakes. The results show that the magma supply rates are almost constant or even decrease with time while the earthquake occurrence rate increases with time. This contrast in their temporal changes is interpreted to result from stress accumulation in the volcanic edifice caused by constant magma supply without effusion of magma to the surface. We further show that data showing slight acceleration in strain can be best explained by magma ascent at a constant velocity, and that there is no evidence for increased magma buoyancy resulting from gas bubble growth. This consideration supports the interpretation that the magma stayed at 2 km depth and horizontally migrated. These findings relating magma supply rate and seismicity to magma ascent process are clues to understanding why no magmatic eruption occurred at Iwate volcano in 1998.

Keywords Magma ascent · Volcano inflation · Strain · Gas bubble growth · Out gassing · Buoyancy

Editorial responsibility: D. Roman

This paper constitutes part of a special issue. The complete citation information is as follows

Nishimura T and Ueki S (2011) Seismicity and magma supply rate of the 1998 failed eruption at Iwate volcano, Japan. In: Moran SC, Newhall CG, Roman DC (eds) Failed eruptions: Late-stage cessation of magma ascent. Bull Volcanol 73(2):133–142

T. Nishimura (✉)
Department of Geophysics, Graduate School of Science,
Tohoku University,
Sendai 980-8578, Japan
e-mail: nishi@zisin.geophys.tohoku.ac.jp

S. Ueki
Research Center for Prediction of Earthquakes and Volcanic Eruptions, Graduate School of Science, Tohoku University,
Sendai 980-8578, Japan

Introduction

The Iwate volcanic group, located in the northeastern region of Japan, is generally classified into two subgroups: The western group (West Iwate) consists of a volcanic edifice characterized by several peaks (Mitsuishi-yama, Inukura-yama, Ohmatsukura-yama, Ubakura-yama and Kurokura-yama) and the eastern group (East Iwate) consists of Yakushi-dake. Onigajo-caldera is located between the western and eastern groups. West Iwate was formed at about 200 ka, and the volcano flank is strongly eroded, whereas East Iwate is a young stratovolcano formed at 5 ka, with the highest peak (2038 m) in East and West Iwate.

There are historical records of large magmatic eruptions at East Iwate (Doi 1991; Ito 1998, 1999). In 1686, an eruption involving scoria emissions, base surges and lahars occurred at the central cone. In 1732, a large amount of basaltic lava was effused from new vents formed on the northeastern flank of East Iwate, forming a flow 3.4 km long with a maximum width of 1.1 km. There are also geological records that indicate two magmatic eruptions, with a debris avalanche on the northeastern flank of East Iwate, between 915 and 1686. The debris

avalanche reached 8 km from the summit, flowing down along a river to Morioka city, which is a capital of Iwate Prefecture with a present-day population of about 260,000. In contrast, there is no historical record of magmatic eruptions at West Iwate, apart from a phreatic eruption in 1919 at Onigajo-caldera. This eruption was small and no damage to human or constructions was reported.

Magmatic eruptions have not occurred at Iwate volcano in the hundreds of years since 1732. During this long dormant period, however, volcanic tremor was first observed in September 1995 (Ueki et al. 1996). After that, volcanic tremor and earthquakes were frequently observed. From February 1998, the seismicity in and around Iwate volcano gradually increased with volcano inflation (Tanaka et al. 2002a), and high seismic activity and volcano inflation continued for about 1 year. The volcano did not finally erupt although a new fumarole field appeared on West Iwate.

We were concerned for a new eruption as the seismic activity became high and the volcano inflated in 1998. The local government organized a working group with scientists to cope with the on-going volcanic activity. The scientists intensively analyzed the seismic and geodetic data to quantitatively evaluate the magma activities and related phenomena, which are summarized in many papers (Miura et al. 2000; Nishimura et al. 2000a, b, 2005; Matsumoto et al. 2001; Uchida et al. 2002; Nakahara et al. 2002; Tanaka et al. 2002a, b; Ueki and Miura 2002; Nakamichi et al. 2003; Yamawaki et al. 2004; Sato and Hamaguchi 2006). It was not known, however, at that time whether the magmatic activity beneath the volcano would lead to volcanic eruptions or finally end as a failed eruption. In the present study, we reexamine the magmatic activity in 1998, giving attention to temporal changes of magma migration as well as the associated seismicity. On the basis of the results reported in previous papers and theoretical consideration on magma ascent process, we investigate the reasons why Iwate volcano failed to erupt in 1998.

Review of volcanic activity in the 1990's

Most of the previous studies on the 1998 volcanic activity depend on the data recorded by geophysical observation networks in and around the volcano. We first briefly summarize the 1998 volcanic activity as well as the observation system.

Permanent geophysical observation was started at Iwate volcano by Tohoku University as a part of the national project for prediction of earthquakes and volcanic eruptions in Japan. Matsukawa station (MTK) was constructed in 1981 about 10 km NW from the summit and consists of a three-component short-period seismometer in a 100 m borehole. In 1994, Ainosawa and Yakebashiri stations (ANS and YKB) were deployed to monitor the volcano with short-period seismometers as well as tilt and strain meters which are set at depths about 300 m beneath the southeast and northeast flanks of East Iwate, respectively. In 1997 Genbudo station (GNB) was constructed on the southwest flank of the volcano with borehole short-period seismometers, and tilt and strain meters. Five Global Positioning System (GPS) stations were established around the volcano by the end of 1996, and eight more stations were deployed between April and August of 1998 (Miura et al. 2000). Short-period and broad-band seismometers were also set at stations around the volcano in 1998 (Nishimura et al. 2000a; Tanaka et al. 2002a). These dense seismic and geodetic networks have succeeded in detecting the 1998 magmatic activity from its initiation to the end.

Figure 1 shows the hypocenters of volcano-tectonic earthquakes, low-frequency earthquakes, the source region of the very-long-period events (Nishimura et al. 2000a; Tanaka et al. 2002a), the locations of the volcanic pressure sources (Sato and Hamaguchi 2006), and the mountain peaks and caldera. The volcanic earthquakes were mainly located between East Iwate and West Iwate, and most of them were at shallow depths less than 5 km. The volcanic pressure sources were also distributed to the east-west. The distributions were elongated almost parallel to the subducting Pacific plate motion direction. The fumarole field that appeared in 1999 was located along the ridge line between Kurokura-yama and Ubakura-yama (Doi et al. 2000).

Spatio-temporal distributions of volcanic pressure sources are reported in detail by Miura et al. (2000) and Sato and Hamaguchi (2006). Miura et al. (2000) located the pressure sources by analyzing the GPS data around the volcano. They showed that the dikes intruded at 3–5 km depths beneath around Inukura-yama from February to April. After that, spherical pressure sources are inferred at about 3–4 km depths beneath around Mitsuishi-yama. These pressure sources migrated westward from February to August. Sato and Hamaguchi (2006) applied a new method using Bayesian decomposition to extract the strain and tilt changes caused by volcanic pressure sources from the raw data, including the effects of sensor installations, influences of rainfall, and secular drifts at the site. Then, they obtain the spatio-temporal distributions of dikes and spherical pressure sources for the eight periods determined from temporal changes observed in strain and tilt data at the three borehole stations (YKB, ANS, and GNB), as well as GPS data at eight stations. Their results show that from February to April, the volcano was mainly inflated by the dikes intruded beneath the Onigajo-caldera, which sometimes propagated westward. Spherical pressure source activity became dominant from May, and was always located at 3 km depth beneath the western flank of the volcano where hydrothermal activity is high. Although there are several differences in the pressure sources determined by Miura et al. (2000) and those by Sato and Hamaguchi (2006), we find that the following main results are indicated in both papers: (1) from February to April, the dike intruded to

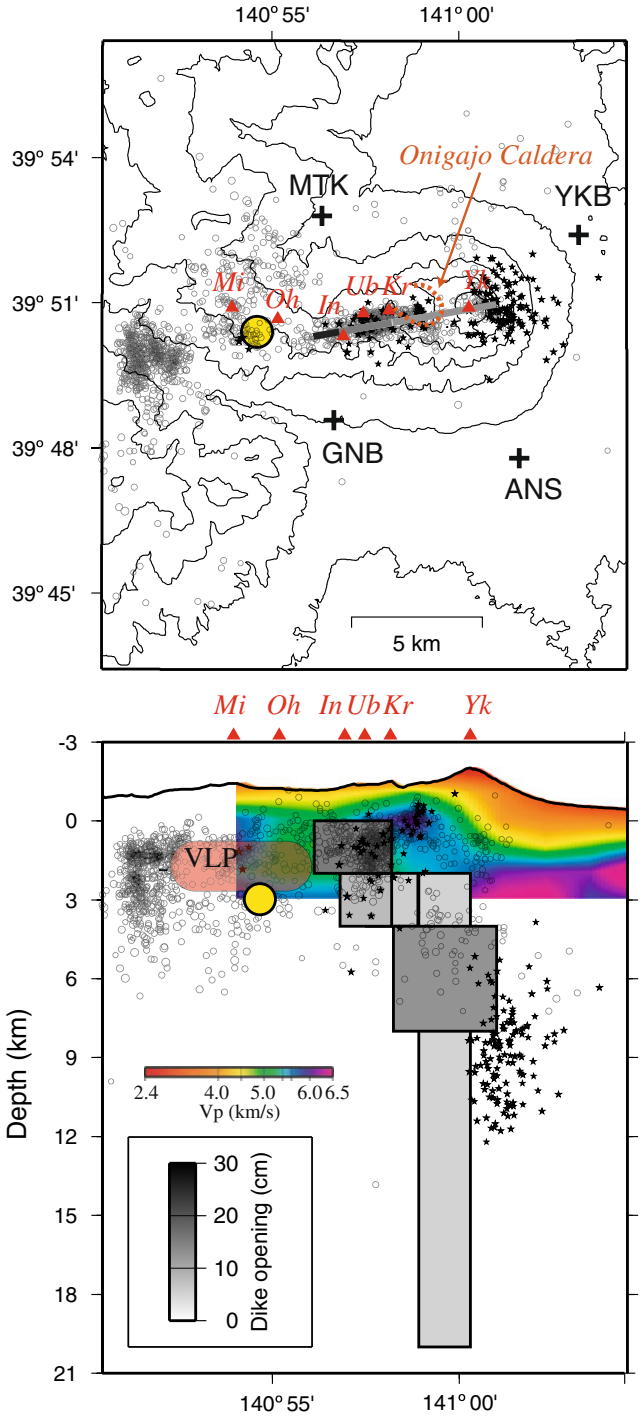

Fig. 1 Spatial distributions of volcanic earthquakes and volcanic pressure sources. Open circles: hypocenters of volcano tectonic earthquakes; solid stars: hypocenters of low-frequency earthquakes; light red color: locations of very-long-period seismic events; yellow circle: the location of the spherical pressure source; grey thick line in map and grey rectangular in the cross section: dikes. Three-dimensional P-wave velocity revealed from an active experiment (Tanaka et al. 2002b) is also shown in the bottom panel. Station locations are denoted by plus symbols. Mountain peaks are indicated by red triangles. *Mi*: Mitsuishi-yama; *Oh*: Ohmatsukura-yama; *In*: Inukura-yama; *Ub*: Ubakura-yama; *Kr*: Kurokura-yama; *Yk*: Yakushidake. Modified from Tanaka et al. (2002b) and Sato and Hamaguchi (2006)

shallow parts beneath from Onigajo-caldera to Ubakura-yama; (2) from May, a spherical pressure source that expanded at shallow parts beneath Mitsuishi-yama was dominant. Both papers also showed that the volcanic pressure source locations are well correlated spatially and temporally with the hypocenters, and the authors suggest that the volcanic earthquakes occurred associated with dike intrusions and spherical pressure source activity at shallow parts.

The time sequence of the 1998 activity of Iwate volcano is divided into four periods below. We briefly summarize the activity.

Before 1998

Volcanic tremor at depths of 8–10 km was first detected beneath East Iwate in September 1995 (Ueki et al. 1996). After that, low-frequency earthquakes and tremor beneath East Iwate were frequently observed. From June 1996, high frequency earthquakes occurred at shallow depths (< 2 km) beneath the summit and flanks of the volcano, and this activity continued until the end of 1997 (Ueki and Miura 2002).

From January to April in 1998

In February 1998, minor volcano inflation of up to 0.1 micro radian per month at the foot of the volcano was observed and shallow volcanic earthquakes occurred (Sato and Hamaguchi 2006). Activity of deep and intermediate-depth low-frequency seismic events likely preceded the shallow volcano-tectonic earthquake activity (Nakamichi et al. 2003). Volcano-tectonic earthquakes and low-frequency earthquakes as well as very-long-period seismic events at shallow depths were observed (Nishimura et al. 2000a; Tanaka et al. 2002a). In the middle of March, a shallow seismic swarm was observed, and at the end of April, more than 100 earthquakes occurred in 1 h (Ueki and Miura 2002). There were dike intrusions at a shallow depth beneath Onigajo-caldera from February to April (Sato and Hamaguchi 2006).

From May to September 2 in 1998

Seismic activity was high from May to July with intense swarms from the end of June to the beginning of July. The very-long-period events at a depth of about 2 km beneath West Iwate were common, with activity highest in late June. The volcanic pressure sources moved to the west and persisted at a shallow depth (~3 km) beneath West Iwate. At the end of August, the shallow seismic activity ceased (Ueki and Miura 2002).

After September in 1998

On September 3, 1998, a M6.1 earthquake occurred at the southwest of Iwate volcano. Stress changes caused by this

earthquake seemed to decrease the seismic activity around Mitsuishi-yama in West Iwate, while the number of earthquakes increased around Onigajo-caldera (Ueki and Miura 2002). There was also a dike intrusion around Onigajo-caldera after the occurrence of the M6.1 earthquake (Sato and Hamaguchi 2006), even though seismic activity gradually decreased as a whole. In March 1999, a new fumarole field and dead plants were found close to Ubakura-yama (Doi et al. 2000). The fumarole field rapidly spread for about 2 km in the east-west direction and 0.5 km in the north-south direction. The fumaroles released about 97% H_2O and 3% CO_2 in August 1999 (Hirabayashi et al. 2006). The activity reached a maximum from January 2000, with fumaroles sometimes 300–500 m high. The activity gradually declined from the latter half of 2001, and had almost ended in July 2004 (Doi and Saito 2005).

Temporal changes in the seismic activity and magma supply rate in 1998

As shown in the previous section, significant magma migration occurred mainly from February to April, and the volcano continued to be inflated after May mainly by the spherical pressure source persistent at a shallow depth beneath West Iwate. After the M6.1 earthquake in September, the volcanic activity gradually decreased. In the present section, we focus on the seismic activity and magma supply rate before the M6.1 earthquake to understand the magmatic activity that did not lead to an eruption.

Figure 2 shows the cumulative and daily numbers of volcanic earthquakes. We count the daily numbers of earthquakes on the monitor paper records, examining S-P times of the short-period seismograms at stations around the volcano. The numbers of earthquakes we counted are larger than those counted from the earthquakes whose hypocenters are determined, which are reported in some previous papers (e.g., Tanaka et al. 2002a; Sato and Hamaguchi 2006). Counting the number of earthquakes on the monitor records has the advantage that we can evaluate the earthquakes whose hypocenters were not determined, and by counting large numbers can capture smooth and/or rapid temporal changes in the activity, although the overall characteristics in temporal changes are not different from each other. Figure 2 indicates that the number of volcanic earthquakes gradually increased from February to August, sometimes indicating swarm activities.

Sato and Hamaguchi (2006) classified the period from February to September 2 into six phases based on the temporal changes in tilt and strain meter data at the three stations. We calculate the magma supply rates from Table 2 in Sato and Hamaguchi (2006) and the earthquake occurrence rates for each phase (Table 1). In Fig. 3, the

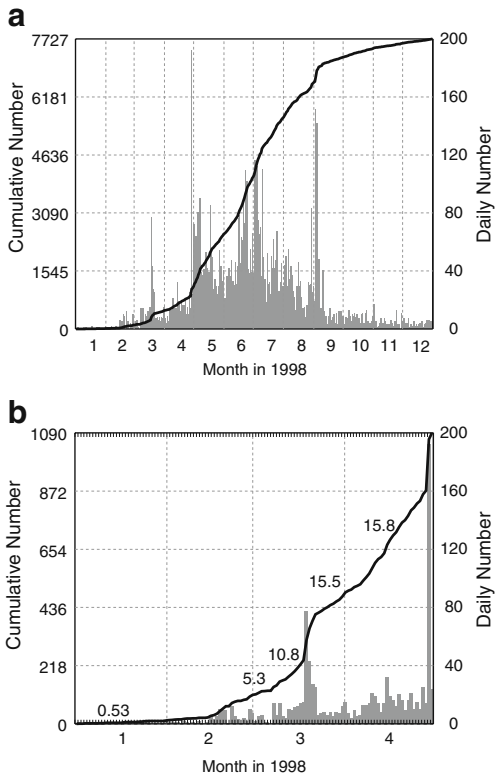

Fig. 2 Cumulative and daily numbers of volcanic earthquakes. **a** From January to December. **b** From January to April. The numbers in (**b**) represent the earthquake occurrence rates per day

magma supply rates obtained for the dike intruded beneath Onigajo-caldera and those for the spherical pressure sources persistent at West Iwate are represented by lines with open squares and open circles, respectively. Total magma supply rates are indicated by lines with solid circles. The magma supply rates obtained from the results in Miura et al. (2000), in which the volcanic pressure sources are determined every 2 months, are shown in Table 2 with the earthquake occurrence rates. They show trends similar to those recognized in Table 1.

We compare the magma supply rates (Fig. 3) and the earthquake occurrence rates (Fig. 2) as well as the spatio-temporal changes of volcanic pressure sources shown in Sato and Hamaguchi (2006). From February 14 to March 12, the magma ascended from a deep region (> 10 km), but the magma intruded horizontally from March 13–18. New magma intrusion at a depth around 6 km was detected from March 19 to April 22. However, the magma did not reach the ground surface, and horizontal intrusion was observed again from April 23–28. The dikes were always located beneath 2 km depth. This observation strongly suggests that the magma was insufficiently buoyant enough to reach the ground surface. In these periods (phases A–D) the occurrence rate of earthquakes increased with time. The occurrence rate was about 0.5 per day from January, but

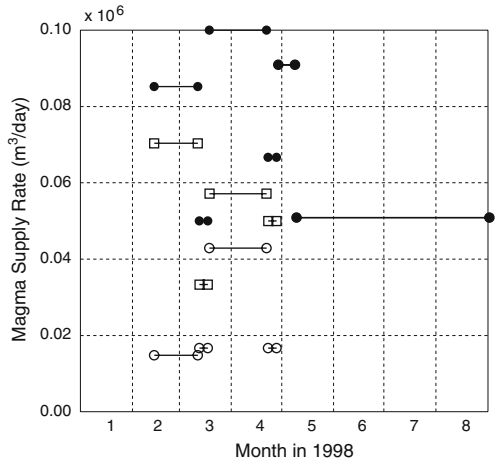

Fig. 3 Temporal changes of magma supply rate estimated from the results of Sato and Hamaguchi (2006). Lines with open squares and circles represent the magma supply rates for the dikes and spherical pressure sources, respectively. Lines with solid circles indicate the total magma supply rates and the observation periods

increased to 5 per day after the middle of February. On March 18, 77 volcanic earthquakes were observed, and then the occurrence rate again increased, more than doubling to 10–16 per day, until the end of April. On the other hand, the magma supply rates of the dike intrusion decreased from 7×10^4 m^3/day in phase A down to about 5×10^4 m^3/day in phases C and D. Total magma supply rates (sum of the rates as the dikes and spherical sources) were almost constant at about $0.85–1.0\times10^4$ m^3/day except when the earthquake swarms occurred. This tendency recognized in the magma supply rate is contrary to that found in the earthquake occurrence rate, which shows gradual increase with time.

After the strong seismic swarm on April 29, the volcano was inflated mainly by the spherical pressure source beneath Mitsuishi-yama (Miura et al. 2000; Sato and Hamaguchi 2006). The spherical pressure source was persistent at the same depth, which is considered to be a buoyancy neutral point. The magma supply rate from the end of April to September 2 (just before the M6.1 earthquake) is estimated to have been 5.1×10^4 m^3/day, which is about half the rate before April 28. Despite this decrease in the magma supply rate, the earthquake occurrence rate in this period increased to more than 40 per day from 5–10 per day before April 28.

The gradual increase in the volcanic earthquake occurrence rate observed at Iwate volcano is often seen at other active volcanoes, and such a temporal change is sometimes considered as a precursor to a new eruption (e.g., McNutt 1996; Voight 1988). The previous papers' results presented here show that the magma supply rates were almost constant or even decreased over the same periods. This contrast in temporal changes may be explained by a similar mechanism of magma accumulation as that presented by Lengliné et al. (2008). To interpret the observed exponential increase of earthquake activity and exponential decay of the volcano deformation rate during the magma accumulation phases at three basaltic volcanoes, Lengliné et al. (2008) uses the results of studies of critical ruptures in heterogeneous media. These studies show that a uniformly increasing stress produces a power law acceleration in cumulative damage of the media near the critical point of rupture. At Iwate volcano, the magma was supplied from greater depth, constantly before May and at a gradually decreasing rate after that, and no eruption occurred. As a result, the stress in the volcanic edifice is considered to have increased with time and gradually decreased after May, which is qualitatively similar to the decay in volcano deformation shown in Lengliné et al. (2008), and consistent with the earthquake occurrence rate increasing with time.

Temporal changes of the observed strain data and magma ascent process

For the case of Iwate volcano, the magmatic activity before April 1998 provides insight into the reasons why Iwate volcano failed to erupt in 1998 and the magma stayed below 2 km. Although Sato and Hamaguchi (2006) determined spatio-temporal distributions of dike intrusions from February to April, the time-resolution in their solutions does not reveal the details of the magma ascent process. In the present study, therefore, we give attention to the temporal changes in the strain data to understand whether or not the magma gained buoyancy during ascent.

Figure 5 in Sato and Hamaguchi (2006) shows that the strain and tilt records are slightly accelerated except during phase B (March 13–18, 1998) from February to April. Sato and Hamaguchi (2006) extracted the signals of volcano inflation by removing a linear trend and exponential decay caused mainly by the sensor installation as well as secular crustal deformation. However, the data series they used (from 1996 or 1998 to 2000) may not be long enough to detrend both the linear and exponential trends, and may cause some artificial bias in the temporal changes in the strain data. To examine the reliability of the temporal changes recognized by Sato and Hamaguchi (2006), we analyze again the data from 1997 to 2009. The dikes intruded beneath Onigajo-caldera are located about 5 km from YKB and ANS stations, and the spherical pressure source that persisted at West Iwate is more than 10 km from these stations. Since the volume increases for the spherical source are less than those for the dikes emplaced before May, these station strains caused by the spherical pressure source are less than one tenth of those caused by the dike. Hence, we analyze the temporal changes of volumetric strain at YKB and ANS stations by applying a dike model. We first

simply de-trend the signals at the two stations by a linear regression estimated by the data from 2005 to 2009, and then subtract an exponential decay obtained from data for the period preceding the 1998 activity (1996–1997). The de-trended strain still shows some trend in the data around the beginning of volcano inflation stages. Hence, we further calculate coefficients of a regression line and an exponential decay for the 1997 data, and extract the linear trend and exponential decay from 1997 to April 1998. The temporal changes in strain obtained by this procedure are shown in Fig. 4. The strains at the two stations fluctuate in 1997 with amplitude of 0.1–0.2 micro strain, and then increase to 0.5–0.7 micro strains from February to April in 1998. The strains also show slightly accelerated changes.

To quantify the accelerated changes in the strain data, we extract the strain data at the two stations for phase A (Feb. 14–Mar. 12) and those for phase C (Mar.19–Apr.22), during which dikes intruded into shallow parts from deep regions. We normalize the amplitude and lapse time of strain data by the maximum amplitude and the total length of each phase, respectively, and plot them on a logarithmic scale (Fig. 5). It is found that the strain amplitudes at the two stations for both phases A and C are almost proportional to the square of the time for the normalized time t' close to 1. The strain

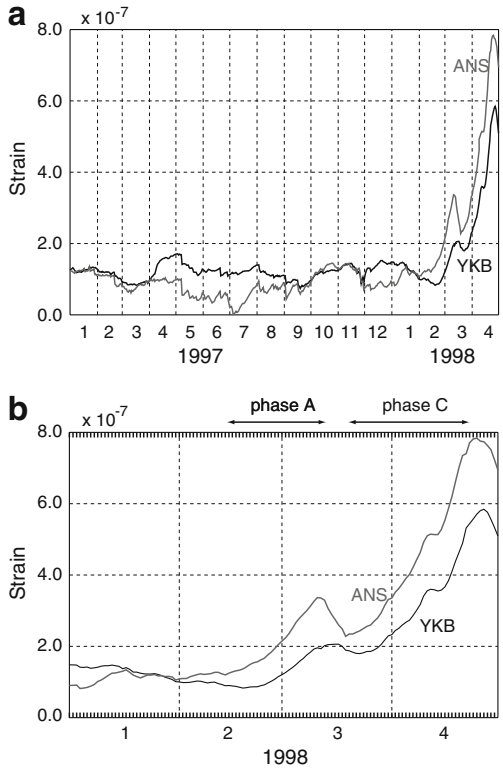

Fig. 4 Temporal changes of volumetric strain data observed by borehole strain meters at YKB and ANS stations. **a** From January 1997 to April 1998. **b** From January to April 1998. Periods of phases A and C in Sato and Hamaguchi (2006) are indicated by arrows on the top of (**b**)

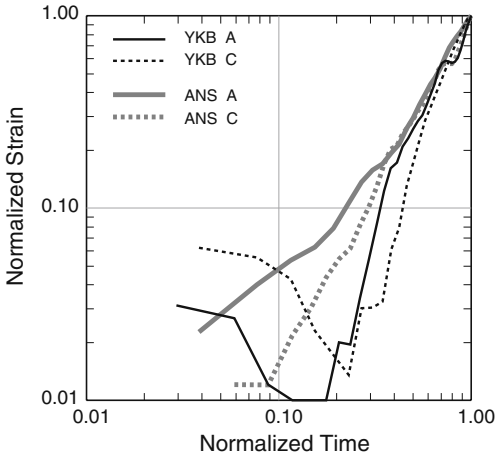

Fig. 5 Logarithmic plot of temporal changes of the normalized strain data at YKB and ANS stations. The strain data for the magma ascent periods (phases A and C) are represented by solid and broken lines, respectively

at YKB seems to increase a little more rapidly than that at ANS, and large differences are also recognized in the temporal changes for ANS and YKB at $t'<0.4$. We do not discuss the detail of these, because noise in the signal may have affected these inflation signals (see Fig. 4).

To understand the observed temporal changes recognized in Fig. 5, we calculate the strains at YKB and ANS for two magma ascent models. The first one is for magma ascent with a constant velocity (constant velocity model). This is a case when the densities of magma and of the surrounding medium are always same. The second model is for ascent of magma with gas bubble growth (gas bubble growth model). The gas bubble growth decreases magma density and generates additional buoyancy in magma, so that possible occurrence of new eruption is considered to become higher. Such a magma ascent process is numerically calculated based on the basic equations of magma flow and gas bubble growth (e.g., Nishimura 2006), but we simply examine the relation of bubble growth to the magma ascent process as follows. The gas bubble growth in melt is characterized by viscous control and diffusion control regimes, but lapse time of the magma ascent from deep parts to shallow depths is so long (i.e., decompression rate is small) that diffusion control is dominant (Toramaru 1995). Hence, the increase in gas bubble radius is proportional to the square root of time (Lyakhovsky et al. 1996). That is, the increase of magma volume is proportional to $t^{1.5}$ (1.5 power of lapse time of magma ascent), where t represents the time. The magma rise speed is proportional to the density difference between the magma and surrounding medium. The density difference $\Delta\rho$ is mainly caused by volume expansion of gas bubbles in magma, $\Delta\rho \cong (M_l + M_g)(V_l^{-1} - (V_l + V_g)^{-1})$, where M and V represent mass and volume, respectively, and

subscripts l and g indicate melt and gas bubbles, respectively. For $V_l >> V_g$, so the density difference is approximated to be $(M_l + M_g)V_l^{-2}V_g$. In this case, therefore, the rise speed is almost proportional to $t^{1.5}$. The volume balance and the rise speed of the magma with gas bubbles give an ascent velocity proportional to $t^{1.5}$ for a constant opening dike width.

For the two models, the length of dike is set to be the same as the best-fit parameters in Sato and Hamaguchi (2006) for phases A (2 km) and C (4 km). For the strike of the dike (N80° E) in Sato and Hamaguchi (2006), the strain calculated at YKB changes more rapidly with time than that at ANS. So, we shift the strike of the dike to N95° E. The bottom depth is not well resolved, so we calculate the strains assuming bottom depths of 12, 16 and 20 km for phase A and 5, 8, 11 km for phase C, respectively, considering the best parameters and their errors in Sato and Hamaguchi (2006). We assume that the dike opening width is constant from the bottom to the top of the magma in the dike. Moving the top of the dike upward with a constant velocity (constant velocity model) or a velocity proportional to the $t^{1.5}$ (gas bubble growth model), we calculate the temporal changes of the strains at the two stations using the formula by Okada (1992) for a homogeneous elastic half space. The calculations are truncated when the top of the dike reaches 2 km depth for phase A and 4 km for phase C, which are the best parameters of Sato and Hamaguchi (2006). Figures 6 shows the temporal changes in strain for phase A at YKB and ANS stations in logarithmic scales, in which the strain amplitudes and lapse times are normalized by the maximum amplitude and lapse time of magma migrating from the bottom to the depth where the magma stops (we call this hereafter the magma ascent time). Comparing the strains for the constant velocity model (Fig. 6a) and gas bubble growth model (Fig. 6b) with the observed data (Fig. 5), we find that the observed strain changes are well explained by the constant velocity model with a bottom depth of 16 km. On the other hand, the strains for the gas bubble growth model rapidly change with time, and even when the bottom depth is set to be shallower down to 12 km from the best solution of 20 km, the predictions deviate from the observations. Figure 7 shows the calculation results for phase C. It is same with the results for phase A; the strains for the gas bubble growth model change more rapidly than those for the constant velocity model. For the constant velocity model, a bottom depth of 11 km is most consistent with the observation. However, even when the bottom depth is set to be 5 km for the gas bubble growth model, which is just 1 km beneath the depth where the dike stops, the predicted strains increase rapidly and do not explain the observed data. These results indicate that the temporal changes of the strain data for phases A and C are better explained by the constant velocity model.

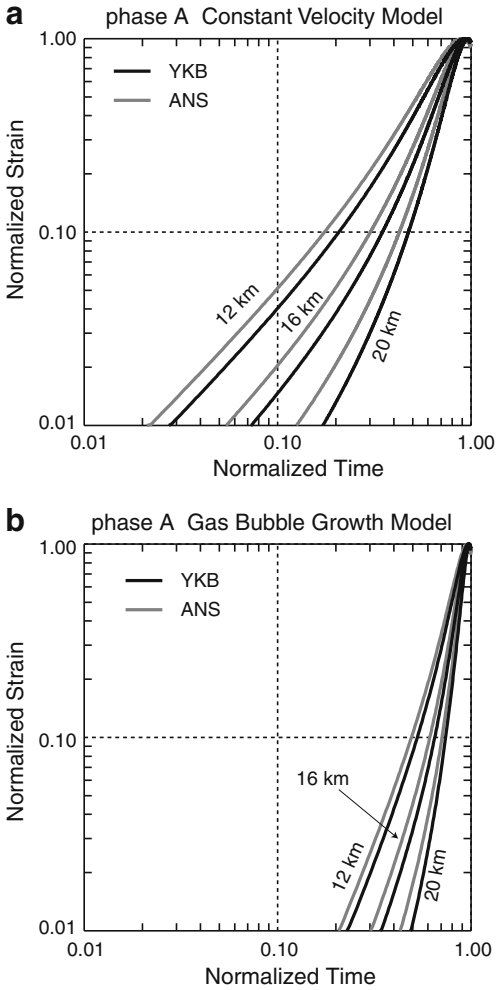

Fig. 6 Logarithmic plot of temporal changes of volumetric strains predicted for the magma ascent for phase A. **a** Constant velocity model. **b** Gas bubble growth model. Three cases for the bottom depth of magma are plotted for each model. See the text for detail

Discussion and conclusions

The considerations in the previous section suggest that the ascending magma did not lower its density during the ascent. Such a magma ascent process may be explained if the magma out-gassed as it ascended. When out-gassing occurs, the gasses in bubbles escape to the country rocks to be dissolved in ground water or to the surface as fumarole, so the magma density does not change much. It is noted that accurate determinations of the rise velocity (or spatio-temporal distribution) of magma are necessary for quantitatively discussing the out-gassing. For example, Shimomura et al. (2006) numerically examined gas bubble growth processes in melt surrounded by an elastic medium by applying a cell model. They show that when the ascending magma is surrounded by a stiff volcanic edifice, the surrounding medium suppresses the growth of gas bubbles and the magma density does not decrease so rapidly. In this case, the

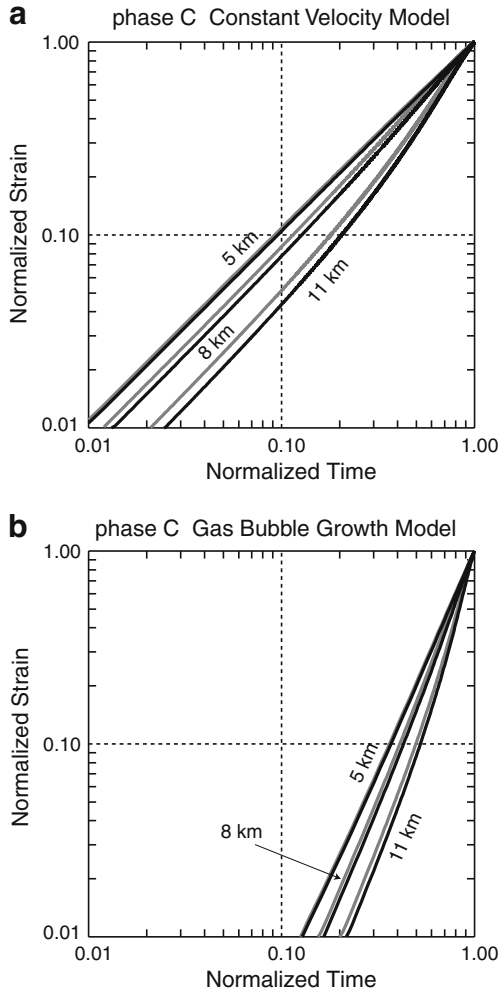

Fig. 7 Logarithmic plot of temporal changes of volumetric strains predicted for the magma ascent for phase C. **a** Constant velocity model. **b** Gas bubble growth model. Three cases for the bottom depth of magma are plotted for each model. See the text for detail

rates of volume increase or density decrease become smaller than in the case of the gas bubble growth model in the previous section, in which the gas bubbles are assumed to freely expand. This implies that even if volatiles are included in magma, the magma rise velocity will be lower compared with the results shown in Figs. 6 and 7.

The rates of strain changes become steeper, plotted on logarithmic scales, with increase in the bottom depth of magma. This is because the lapse time and amplitude of the strain data are normalized by the magma ascent time and the maximum amplitude, respectively. The magma ascent time increases as the bottom depth of magma becomes deeper. On the other hand, the strain amplitude is strongly affected by the dike opening around the depths where the ascending magma stops. Therefore, it is quite important to accurately determine the bottom depth of the magma for comparing the theoretical predictions with the observed strains in logarithmic scale. If the bottom depths of magma were much more accurately determined for phases A and C, and data with high signal-to-noise ratios were available, we could discuss the details of magma ascent process; for example, the starting depths and volumes of gas bubble growth and out-gassing, and effects of the surrounding medium.

We have not included the visco-elasticity of the structure in interpreting the observed seismicity and magma supply rate or calculation of the strain in the two magma ascent models. Viscosity of the medium, especially around a reservoir and conduit, may introduce some time delays in deformation and stress field response. Hence, evaluating this effect is necessary for examining the temporal changes in seismicity and volcano deformation. Looking for example at the deformation data for Sakurajima volcano, Japan, where magma is constantly supplied from deeper parts and Vulcanian explosions frequently occur for decades, volcano inflations occur several hours before each explosive eruption, and the source depth of inflation is estimated to be about 2–6 km (Ishihara 1990). This observation suggests that the time delay originating from viscosity of the medium surrounding magma is not so long, probably less than 1 h, which is much shorter than the temporal changes of seismicity and volcano deformation at Iwate volcano we discussed in this paper. However, this observation is not obtained for Iwate volcano and further quantitative discussion may be necessary for detailed analyses. Some time delays may be seen in the strain data at YKB for those at ANS, especially in the middle of March. However, signal to noise ratios of these data are low so that we do not discuss the difference in detail.

Aizawa et al. (2009) analyze MT data and find a high-resistivity zone beneath Onigajo-caldera at a depth about 2 km and interpret the zone as old, solidified magma. Comparing their results with the spatio-temporal distributions of dikes and volcanic pressure sources (Sato and Hamaguchi 2006), a high P-wave velocity (Tanaka et al. 2002a) and high Bouger anomaly zone beneath Onigajo-caldera (Tanaka et al. 2002b), they infer that the old solidified magma impeded the magma ascent and forced a partial migration of the magma to the west. Such structural controls by solidified magma are often observed on eastern Izu Peninsula (Hayashi and Morita 2003). On the other hand, horizontal migration during magma ascent is also predicted from numerical calculations (e.g., Taisne and Jaupart 2009) when the magma encounters a lower density zone of a sufficient thickness. Nakagawa and Togari (1999) pointed out the existence of a density barrier for basaltic magma beneath West Iwate, which helps explain why the spherical pressure sources persisted beneath West Iwate. Since the results in the previous section indicate that the magma does not gain additional buoyancy by the time when it encounters the solidified magma around 2 km,

mapping the detailed density structure is a key to understand which mechanism is dominant for the horizontal migration of the 1998 Iwate volcano case; the structural control by the solidified magma or the density barrier.

We reconcile the spatio-temporal distributions of pressure sources in the previous papers with the daily numbers of volcanic earthquakes. We further examine two basic magma ascent models to understand the temporal changes in the observed strain data. The main results are summarized as follows. The earthquake occurrence rate gradually increased from the initiation of the 1998 volcanic activity, while the magma supply rates were almost constant or even decreased with time over the same period. This difference in trends can be qualitatively interpreted by considering that the stress accumulation in the volcanic edifice was caused by the magma staying at shallow depth. The observed strain data at YKB and ANS stations before May are almost proportional to the square of lapse time, which is not explained by magma ascent accompanied by gas bubble growth in melt. This implies that the magma could not gain sufficient additional buoyancy to reach the ground surface. This may be one reason why Iwate volcano failed to erupt in 1998.

Acknowledgements We thank Minemori Sato for his help on arrangement of the strain data at Iwate volcano. We are grateful to Diana Roman, Seth Moran and Chris Newhall for their editorial efforts on this special issue. Careful reviews by two anonymous reviewers improved this manuscript. This study was partly supported by the Ministry of Education, Culture, Sports, Science and Technology (MEXT) of Japan, under its Observation and Research Program for Prediction of Earthquakes and Volcanic Eruptions.

References

Aizawa K, Ogawa Y, Mishina M, Takahashi K, Nagaoka S, Takagi N, Sakanaka S, Miura T (2009) Structural controls on the 1998 volcanic unrest at Iwate volcano: Relationship between a shallow, electrically resistive body and the possible ascent route of magmatic fluid. J Volcanol Geotherm Res 187:131–139

Doi N (1991) Debris avalanche deposits at the foot of Iwate volcano, Northeast Japan. Bull Volcano Soc Jp 36:483–484, in Japanese with English abstract

Doi N and Saito T (2005) Summary of the activity of Iwate volcano and details of volcano disaster prevention measures. Chapter 1 in Records for the 1998 eruption crisis of Iwate volcano (edited by Doi N, Kikuchi S, Yoshida K), Iwate Office of River and National Highway, The Tohoku Regional Bureau, The Ministry of Land, Infrastructure and Transport, and Iwate Prefecture (in Japanese)

Doi N, Saito T, Doi S, Numakunai T (2000) Fumarolic activity in West Iwate volcano from 1999 to 2000. Japan Earth and Planetary Science Joint Meeting 2000, Vb-p002

Hayashi Y, Morita Y (2003) An image of a magma intrusion process inferred from precise hypocentral migrations of earthquake swarm east of Izu Peninsula. Geophys J Int 153:159–174

Hirabayashi, J, Nogami K, Ohba, T (2006) Relationship between chemical composition of volcanic gases and volcanic activity at Mt. Iwate, Japan. In *Report on the Joint Observation of Iwate Volcano in 1999*: 137–147 (in Japanese with English abstract)

Ishihara K (1990) Pressure sources and induced ground deformation associated with explosive eruptions at an andesitic volcano: Sakurajima volcano, Japan. In: Ryan M (ed) Magma Transport and Storage. Wiley, Chichester, pp 335–356

Ito J (1998) The Eruption History of Iwate Volcano in the Edo Period, based on the Historical Documents. Bull Volcano Soc Jp 43:467–481 (in Japanese with English abstract)

Ito J (1999) Eruption sequence and ^{14}C Age of phreatic Eruptions occured at West Iwate Volcano in historic age. Bull Volcano Soc Jp 44:261–266 (in Japanese with English abstract)

Lengliné O, Marsan D, Got J-L, Pinel V, Ferrazzini V, Okubo P G (2008) Seismicity and deformation induced by magma accumulation at three basaltic volcanoes. J Geophys Res 113: doi:10.1029/2008JB005937

Lyakhovsky V, Hurwitz S, Navon O (1996) Bubble growth in rhyolitic melts: Experimental and numerical investigation. Bull Volcanol 58:19–32

Matsumoto S, Obara K, Yoshimoto K, Saito T, Ito A, Hasegawa A (2001) Temporal change in P-wave scatter distribution associated with the M6.1 earthquake near Iwate volcano, northeastern Japan. Geophys J Int 145:48–58

McNutt S (1996) Seismic monitoring and eruption forecasting of volcanoes: A review of the state-of-the-art and case histories. In: Scarpa R, Tilling RI (eds) Monitoring and Mitigation of Volcano Hazards. Springer, Berlin, p 841, 99–146

Miura S, Ueki S, Sato T, Tachibana K, Hamaguchi H (2000) Crustal deformation associated with the 1998 seismo-volcanic crisis of Iwate Volcano, Northeastern Japan, as observed by a dense GPS network. Earth Planet Space 52:1003–1008

Nakagawa M, Togari H (1999) Iwate volcano from a petrological point of view: Magma plumbing system and some characteristics of the acitity. Chokyu Monthly 239:264–268

Nakahara H, Nishimura T, Sato H, Ohtake M, Kinoshita S, Hamaguchi H (2002) Broad-band source process of the 1998 Iwate Prefecture, Japan, earthquakes as revealed from inversion analyses of seismic waveforms and envelopes. Bull Soc Seis Am, ( ) 92:1708–1720

Nakamichi H, Hamaguchi H, Tanaka S, Ueki S, Nishimura T, Hasegawa A (2003) Source mechanisms of deep and intermediate-depth low-frequency earthquakes beneath Iwate volcano, northeastern Japan. Geophys J Int 154:811–828

Nishimura T (2006) Ground deformation due to magma ascent with and without degassing. Geophys Res Lett 33:L23309. doi:10.1029/2006GL028101

Nishimura T, Nakamichi H, Tanaka S, Sato M, Kobayashi T, Ueki S, Hamaguchi H, Ohtake M, Sato H (2000a) Source process of very long period seismic events associated with the 1998 activity of Iwate Volcano, northeastern Japan. J Geophys Res 105:19135–19147

Nishimura T, Uchida N, Sato H, Ohtake M, Tanaka S, Hamaguchi H (2000b) Temporal changes of the crustal structure associated with the M6.1earthquake on September 3, 1998, and the volcanic activity of Mount Iwate, Japan. Geophys Res Lett 27:269–272

Nishimura T, Tanaka S, Yamawaki T, Yamamoto H, Sano T, Sato M, Nakahara H, Uchida N, Hori S, Sato H (2005) Temporal changes in seismic velocity of the crust around Iwate volcano, Japan, as inferred from analyses of repeated active seismic experiment data from 1998 to 2003. Earth Planets Space 57:491–505

Okada Y (1992) Internal deformation due to shear and tensile faults in a half-space. Bull Seism Soc Am 82:1018–1040

Sato M, Hamaguchi H (2006) Weak long-lived ground deformation related to Iwate volcanism revealed by Bayesian decomposition of strain, tilt and positioning data. J Volcanol Geotherm Res 155:244–262

Shimomura Y, Nishimura T, Sato H (2006) Bubble growth processes in magma surrounded by an elastic medium. J Volcanol Geotherm Res 155:307–322

Taisne B, Jaupart C (2009) Dike propagation through layered rocks. J Geophys Res 114:B09203. doi:10.1029/2008JB006228

Tanaka S, Hamaguchi H, Ueki S, Sato M, Nakamichi H (2002a) Migration of seismic activity during the 1998 volcanic unrest at Iwate volcano, northeastern Japan, with reference to P and S wave velocity anomaly and crustal deformation. J Volcanol Geotherm Res 113:399–414

Tanaka S, Hamaguchi H, Nishimura T, Yamawaki T, Ueki S, Nakamichi H, Tsutsui T, Miyamachi H, Matsuwo N, Oikawa J, Ohminato T, Miyaoka K, Onizawa S, Mori T, Aizawa K (2002b) Three-dimensional P-wave velocity structure of Iwate volcano, Japan from active seismic survey. Geophys Res Lett 29: doi:10.1029/2002GL014983

Toramaru A (1995) Numerical study of nucleation and growth of bubbles in viscous magmas. J Geophys Res 100:1913–1931

Uchida N, Nishimura T, Yoshimoto K, Nakahara H, Sato H, Ohtake M, Tanaka S, Hamaguchi H (2002) Temporal change of seismic-wave velocity associated with the 1998 northern Iwate prefecture. Japan earthquake. J Seismol Soc Jpn (Zisin) 55:193–206 (in Japanese with English abstract)

Ueki S, Miura S (2002) Volcanic and seismic activities observed around Iwate volcano in 1998. J Geography 111:154–165 (in Japanese with English abstract)

Ueki S, Morita Y, Hamaguchi H (1996) On the volcanic tremor observed at Iwate Volcanoi in September and October, 1995. Tohoku J Natural Disas Sci 32:258–292 (in Japanese)

Yamawaki T, Nishimura T, Hamaguchi H (2004) Temporal change of seismic structure around Iwate volcano inferred from waveform correlation analysis of similar earthquakes. Geophys Res Lett 31: doi:10.1029/2004GL021103

Voight B (1988) A method for prediction of volcanic eruptions. Nature 332:125–130